Biochemical and Biophysical Research Communications 422 (2012) 219–223

Contents lists available at SciVerse ScienceDirect

Biochemical and Biophysical Research Communications

journal homepage: www.elsevier.com/locate/ybbrc

Pseudo-enzymatic hydrolysis of 4-nitrophenyl myristate by human serum albumin

Paolo Ascenzi [a,b,*], Mauro Fasano [c]

[a] Interdepartmental Laboratory of Electron Microscopy, University Roma Tre, Via della Vasca Navale 79, I-00146 Roma, Italy
[b] National Institute of Biostructures and Biosystems, Viale Medaglie d'Oro 305, I-00136 Roma, Italy
[c] Department of Theoretical and Applied Sciences – Biomedical Research Division, and Center of Neuroscience, University of Insubria, Via Alberto da Giussano 12, I-21052 Busto Arsizio (VA), Italy

ARTICLE INFO

Article history:
Received 13 April 2012
Available online 27 April 2012

Keywords:
Human serum albumin
4-Nitrophenyl myristate
Pseudo-enzymatic hydrolysis
pH effects

ABSTRACT

Most of the esterase properties of human serum albumin (HSA) are the result of multiple irreversible chemical modifications rather than turnover. The HSA-catalyzed hydrolysis of 4-nitrophenyl myristate (NphOMy) is consistent with the minimum three-step mechanism involving the acyl-enzyme intermediate HSA-OMy:

$$\mathrm{HSA} + \mathrm{NphOMy} \underset{k_{-1}}{\overset{k_{+1}}{\rightleftarrows}} \mathrm{HSA{:}NphOMy} \underset{k_{-2}}{\overset{k_{+2}}{\rightleftarrows}} \mathrm{HSA{-}OMy} \underset{+\mathrm{NphOH}}{\overset{k_{+3}}{\rightleftarrows}} \mathrm{HSA} + \mathrm{MyOH}$$

Under all the experimental conditions, values of K_s (= k_{-1}/k_{+1}), k_{+2}, and k_{+2}/K_s determined under conditions where [HSA] $\geqslant 5 \times$ [NphOMy] and [NphOMy] $\geqslant 5 \times$ [HSA] match very well each other. The deacylation process is rate limiting in catalysis (*i.e.*, $k_{+3} \ll k_{+2}$) and $k_{-2} \sim k_{-3} \sim 0\ s^{-1}$. The pH dependence of k_{+2}/K_s, k_{+2}, and K_s reflects the acidic pK_a-shift of one ionizing group from 8.9 ± 0.2 in NphOMy-free HSA to 6.8 ± 0.3 in the HSA:NphOMy adduct. The HSA-catalyzed hydrolysis of NphOMy is inhibited competitively by diazepam, indicating that Tyr411 is the active-site nucleophile.

1. Introduction

Human serum albumin (HSA), the most abundant protein in plasma (*ca.* 7×10^{-4} M) represents the main determinant of plasma oncotic pressure and the main modulator of fluid distribution within the body compartments. Moreover, HSA displays an extraordinary ligand-binding capacity, providing a depot and carrier for many endogenous and exogenous compounds, affecting pharmacokinetics of many drugs, inducing the metabolic modification(s) of some ligands, rendering potential toxins harmless, accounting for most of the anti-oxidant capacity of human plasma, and displaying (pseudo-)enzymatic properties [1–5].

HSA is an all α-helical protein arranged in a globular heart-shaped conformation containing three homologous domains (named I, II, and III); each domain consists of two separate subdomains (named A and B) [2,4,5]. The multidomain organization of HSA is at the root of its capability to bind not only endogenous and exogenous low molecular weight compounds but also peptides and proteins at multiple sites [1–5]. Moreover, HSA displays (pseudo-)enzymatic properties, most of which (*e.g.*, the esterase activity) being the result of multiple irreversible chemical modifications rather than of the catalytic activity occurring at a single reactive site [5,6]. Remarkably, the apparent HSA-catalyzed hydrolysis of the acylating agent 4-nitrophenyl acetate is the result of the irreversible acetylation of 82 residues (*i.e.*, 59 Lys, 10 Ser, 8 Thr, 4 Tyr, and Asp1) rather than of turnover [6].

Here, kinetics of the HSA-catalyzed hydrolysis of 4-nitrophenyl myristate (NphOMy), obtained under conditions where [HSA] $\geqslant 5 \times$ [NphOMy] and [NphOMy] $\geqslant 5 \times$ [HSA] (between pH 6.9 and 9.5, at 22.0 °C), are reported. The Tyr411 residue, located at the FA3-FA4 cleft, represents the catalytic center of HSA. Moreover, the acid–base equilibrium of Tyr411 modulates the HSA pseudo-enzymatic activity.

2. Materials and methods

HSA, NphOMy, diazepam, 4-nitrophenol (NphOH), bis(2-hydroxyethyl)amino–tris(hydroxymethyl)methane (Bis–Tris), 4-(2-hydroxyethyl)-1-piperazineethanesulfonic acid (Hepes),

Abbreviations: AMPSO, 3-[(1,1-dimethyl-2-hydroxyethyl)amino]-2-hydroxypropanesulfonic acid; Bis–Tris, bis(2-hydroxyethyl)amino–tris(hydroxymethyl)methane; Hepes, 4-(2-hydroxyethyl)-1-piperazineethanesulfonic acid; HSA, human serum albumin; MyOH, myristic acid; NphOH, 4-nitrophenol; NphOMy, 4-nitrophenyl myristate.

* Corresponding author at: Interdepartmental Laboratory of Electron Microscopy, University Roma Tre, Via della Vasca Navale 79, I-00146 Roma, Italy. Fax: +39 06 5733 6321.
E-mail address: ascenzi@uniroma3.it (P. Ascenzi).

0006-291X/$ - see front matter © 2012 Elsevier Inc. All rights reserved.
http://dx.doi.org/10.1016/j.bbrc.2012.04.111

3-[(1,1-dimethyl-2-hydroxyethyl)amino]-2-hydroxypropanesulfic acid (AMPSO), and 2-amino-2-methyl-1-propanol were obtained from Sigma–Aldrich (St. Louis, MO, USA). All chemicals were of analytical or reagent grade and were used without further purification.

HSA (from Sigma–Aldrich, St. Louis, MO, USA) was essentially fatty acid free, according to the charcoal delipidation protocol [7–9], and was used without further purification. The HSA stock solution ([HSA] = 5.0×10^{-3} M) was prepared by dissolving HSA in 1.0×10^{-2} M phosphate buffer pH 7.0, at 22.0 °C. The HSA concentration was determined spectrophotometrically at 279 nm ($\varepsilon = 3.6 \times 10^4$ M^{-1} cm^{-1}) [1]. Then, the HSA stock solution was diluted in the desired buffer (Bis–Tris buffer, pH 6.9–7.2; Hepes buffer, pH 6.9–8.2; AMPSO buffer, pH 8.3–9.5; all 0.1 M); the final pH ranged between 6.9 and 9.5. The final HSA concentration ranged between 2.0×10^{-6} and 2.0×10^{-4} M.

The NphOMy solution was prepared by dissolving the substrate in a 3.0×10^{-3} M Bis–Tris buffer solution (pH 6.9) in the presence of 10% acetonitrile. The NphOMy concentration was determined spectrophotometrically at 400 nm ($\varepsilon = 1.8 \times 10^4$ M^{-1} cm^{-1}; pH > 8.5 and 22.0 °C) quantitating NphOH released from the substrate [10]. The final NphOMy concentration ranged between 2.0×10^{-6} and 2.0×10^{-4} M. The final acetonitrile concentration was 1% (v/v) [11].

Kinetics of the HSA-catalyzed hydrolysis of NphOMy was followed spectrophotometrically between 350 nm and 450 nm by rapid-mixing the HSA and NphOMy solutions [10,11].

Values of kinetic parameters obtained under conditions where [NphOMy] ⩾ 5 × [HSA] and [HSA] ⩾ 5 × [NphOMy], between pH 6.9 and 9.5 at 22.0 °C, were analyzed in the framework of the minimum three step-mechanism reported in Scheme 1 (see [6,10–13]).

In Scheme 1, HSA-OMy could be an ester formed between the acyl moiety of the substrate and the phenoxyl oxygen atom of Tyr411 (see [6]), NphOH is 4-nitrophenol, MyOH is myristic acid, k_{+1} is the second-order rate constant for the formation of the HSA:NphOMy complex starting from HSA and NphOMy, k_{-1} is the first-order rate constant for the dissociation of the HSA:NphOMy complex to HSA and NphOMy, K_s (= k_{-1}/k_{+1}) is the pre-equilibrium constant, k_{+2} is the first-order acylation rate constant, k_{-2} is the first-order rate constant for the conversion of the HSA-OMy adduct to the HSA:NphOMy complex, k_{+3} is the first-order deacylation rate constant, and k_{-3} is the second-order rate constant for the formation of the HSA-OMy adduct starting from HSA and MyOH.

Kinetics of the HSA-catalyzed hydrolysis of NphOMy were analyzed using the GraphPad Prism program (GraphPad Software Inc., La Jolla, CA, USA). The results are given as mean values of at least four experiments plus or minus the corresponding standard deviation.

3. Results and discussion

The determination of the kinetic parameters of Scheme 1 is simplified by the fact that the formation of the HSA:NphOMy complex can be treated as a rapid equilibrium process (*i.e.*, $k_{-1} \gg k_{+2}$), under all the experimental conditions. In fact: (*i*) no lag phase occurs in the release of NphOH from NphOMy in the presence of HSA (see Fig. 1), and (*ii*) the equilibration of HSA:NphOMy with HSA and NphOMy is complete within 1.1×10^{-3} s (*i.e.*, the "dead-time" of the rapid-mixing stopped-flow apparatus; $k^{exp} = k_{+1} \times [HSA] = k_{+1} \times [NphOMy] \geqslant 4 \times 10^3$ s^{-1}). Therefore, given that values of K_s (=k_{-1}/k_{+1}) for NphOMy binding to HSA range between $(7.2 \pm 0.7) \times 10^{-5}$ M and $(1.6 \pm 0.1) \times 10^{-6}$ M (see Table 1), it follows that $k_{+1} = k^{exp}/[HSA] = k^{exp}/[NphOMy] \geqslant 2 \times 10^8$ M^{-1} s^{-1} and $k_{-1} \geqslant 1 \times 10^4$ s^{-1}. Remarkably, values of k_{+2} range between $(1.3 \pm 0.1) \times 10^{-4}$ s^{-1} and $(2.6 \pm 0.3) \times 10^{-4}$ s^{-1} (see Table 1). Moreover, the rate of NphOH release from NphOMy catalyzed by HSA is unaffected by the addition of NphOH (up to 1.0×10^{-4} M) in the reaction mixtures, indicating that k_{-2} and k_{-3} approximate to 0 s^{-1}.

When [HSA] ⩾ 5 × [NphOMy], with $k_{-1} \gg k_{+2}$, the rate of NphOH release from NphOMy is a first-order process (Fig. 1, panel A) with a pseudo-first order rate constant (*i.e.*, k_{app}), according to Eq. (1) [10–13]:

$$k_{app} = (k_{+2} \times [HSA])/(K_s + [HSA]) \quad (1)$$

The reaction of HSA with NphOMy is a first-order process for more than 90% of its course (Fig. 1, panel A) and values of k_{app} are independent of the observation wavelength over the whole range explored (*i.e.*, between 350 and 450 nm) at fixed NphOMy concentration. Moreover, values of k_{app} are independent of the NphOMy concentration when [HSA] ⩾ 5 × [NphOMy]. Values of k_{+2} and K_s (see Table 1) were determined by Eq. (1) from hyperbolic plots of k_{app} versus [HSA], as shown in Fig. 1 (panel B).

When [NphOMy] ⩾ 5 × [HSA], a mono-exponential time course is observed (Fig. 1, panel C). Under conditions where $k_{+2} \geqslant 5 \times k_{+3}$, the differential equations arising from Scheme 1 may be solved [12,13] to describe the NphOH release in the early stages of the reaction. The resulting expression is given in Eqs. (2)–(4) [12,13]:

$$[P_1] = \{(k_{cat} \times [HSA] \times [NphOMy] \times t)/(K_m + [NphOMy])\} + \alpha \times [HSA] \times (1 - e^{-kobs \times t}) \quad (2)$$

where

$$\alpha = \{(k_{+2} \times [NphOMy])/((k_{+2} + k_{+3}) \times (K_m + [NphOMy]))\}^2 \quad (3)$$

and

$$k_{obs} = (k_{+2} \times [NphOMy])/(K_s + [NphOMy]) + k_{+3} \quad (4)$$

As predicted from Eqs. (2)–(4), a "burst" phase of NphOH release of amplitude $\alpha \times [HSA]$ with the first order rate constant k_{obs} occurs at all pH values explored. Values of the relative amplitude of the "burst" phase, obtained at [NphOMy] ⩾ 5 × [HSA], range between 0.96 and 1.04, the average amplitude of the "burst" phase is 1.00 ± 0.04. This indicates that the HSA:NphOMy:NphOH stoichiometry is 1:1:1. Moreover, the time course of the "burst" phase of NphOH release is a first-order process for more than 90% of its course (Fig. 1, panel C) and values of k_{obs} are independent of the observation wavelength over the whole range explored (*i.e.*, between 350 and 450 nm) at fixed HSA concentration. Values of k_{obs} are independent of the HSA concentration when [NphOMy] ⩾ 5 × [HSA]. Values of k_{+2} and K_s (see Table 1) were determined by Eq. (4) from hyperbolic plots of k_{obs} versus [NphOMy], as shown in Fig. 1 (panel D). Under all the experimental conditions, the value of k_{+3} is at least 10-fold smaller than the k_{obs} value obtained at the lowest NphOMy concentration (i.e., $k_{+3} < 10^{-6}$ s^{-1}). Thus, the deacylation process (*i.e.*, k_{+3}) is rate limiting in the HSA-catalyzed hydrolysis of NphOMy.

As predicted by Scheme 1, values of K_s and k_{+2} obtained under conditions where [HSA] ⩾ 5 × [NphOMy] from Eq. (1) are in excellent agreement with those obtained under conditions where [NphOMy] ⩾ 5 × [HSA] from Eq. (4) (see Table 1). Moreover, no evidence of a steady-state process was observed, NphOMy acting as a "suicide substrate".

Although the Tyr411 residue, located at the FA3-FA4 cleft, is the primary catalytic center for the HSA-catalyzed hydrolysis of 4-

$$\text{HSA} + \text{NphOMy} \underset{k_{-1}}{\overset{k_{+1}}{\rightleftharpoons}} \text{HSA:NphOMy} \underset{k_{-2}}{\overset{k_{+2}}{\rightleftharpoons}} \text{HSA-OMy} + \text{NphOH} \overset{k_{+3}}{\rightleftharpoons} \text{HSA} + \text{MyOH}$$

Scheme 1.

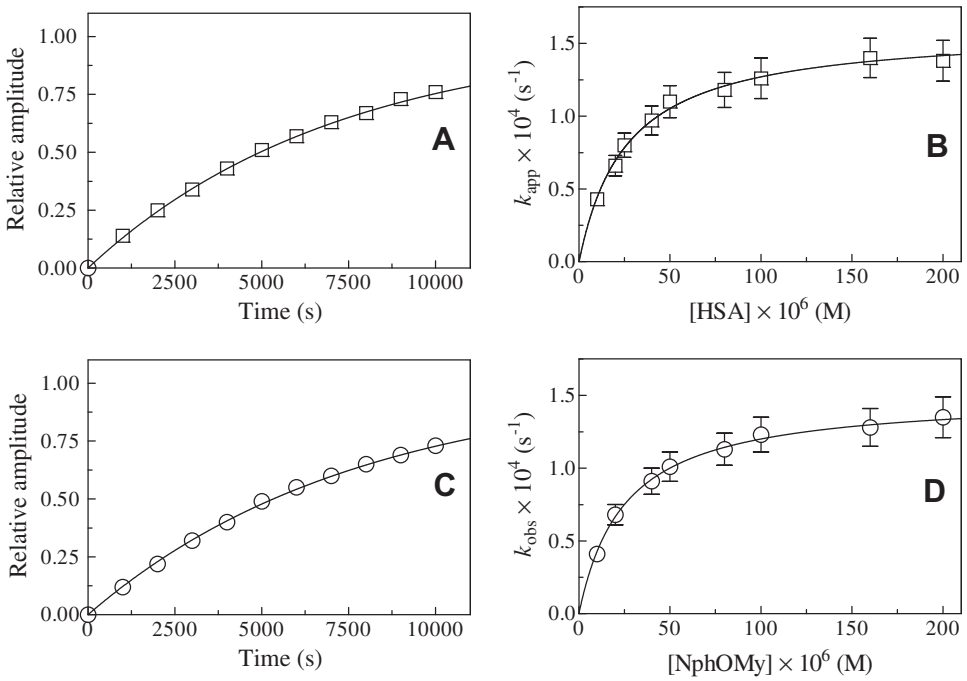

Fig. 1. HSA-catalyzed hydrolysis of NphOMy, at pH 7.5 and 22.0 °C. (Panel A) Time course of the reaction of 2.0×10^{-4} M HSA with 2.0×10^{-6} M NphOMy, *i.e.* [HSA] ⩾ 5 × [NphOMy]. The continuous line was calculated according to the following equation:
$[NphOMy]_t = [NphOMy]_i \times (1 - e^{-kapp \times t})$
with $k_{app} = 1.4 \times 10^{-4}$ s^{-1}. (Panel B) Dependence of k_{app} on the HSA concentration at [HSA] ⩾ 5 × [NphOMy]. The continuous line was obtained according to Eq. (1) with the following parameters $k_{+2} = (1.6 \pm 0.2) \times 10^{-4}$ s^{-1} and $K_s = (2.6 \pm 0.3) \times 10^{-5}$ M. [NphOMy] was 2.0×10^{-6} M and [HSA] ranged between 1.0×10^{-5} and 2.0×10^{-4} M. (Panel C) Time course of the reaction of 2.0×10^{-4} M NphOMy with 2.0×10^{-6} M HSA, *i.e.* [NphOMy] ⩾ 5 × [HSA]. The continuous line was calculated according to the following equation:
$[NphOMy]_t = [NphOMy]_i \times (1 - e^{-kobs \times t})$
with $k_{obs} = 1.3 \times 10^{-4}$ s^{-1}. (Panel D) Dependence of k_{obs} on the NphOMy concentration at [NphOMy] ⩾ 5 × [HSA]. The continuous line was obtained according to Eq. (4) with the following parameters $k_{+2} = (1.5 \pm 0.2) \times 10^{-4}$ s^{-1} and $K_s = (2.5 \pm 0.3) \times 10^{-5}$ M. The value of k_{+3} approximates to 0 s^{-1}. [HSA] was 2.0×10^{-6} M, and [NphOMy] ranged between 1.0×10^{-5} and 2.0×10^{-4} M. For details, see text.

nitrophenyl acetate [6,11], no evidences are available concerning the primary esterase site for the HSA-catalyzed hydrolysis NphOMy. In fact, myristate binds to several HSA sites including the FA3-FA4 cleft [14,15]. Therefore, the inhibitory effect of diazepam, binding selectively to the FA3-FA4 cleft [16], on the HSA-catalyzed hydrolysis of NphOMy has been investigated.

As expected for the pure competitive inhibition mechanism [17], values of the K_s^{app}/K_s ratio (K_s^{app} indicates K_s values obtained in the presence of diazepam) for the HSA-catalyzed hydrolysis of NphOMy, obtained at [HSA] ⩾ 5 × [NphOMy], increase with the diazepam concentration (*i.e.*, [diazepam]; Fig. 2), whereas values of k_{+2} are unaffected by the drug (data not shown). The analysis of data according to Eq. (5) [17]:

$$K_s^{app}/K_s = (1/K_I) \times [\text{diazepam}] + 1 \quad (5)$$

allowed to determine the value of the equilibrium constant for diazepam binding to HSA (*i.e.*, $K_I = 1.0 \times 10^{-5}$ M, at pH 7.5 and 22.0 °C). The value of K_I here determined agrees with that reported in the literature ($K_I = 1.1 \times 10^{-5}$ M, at pH 7.2 and 25.0 °C) [18]. These data indicate that the FA3-FA4 cleft is not only the primary esterase site for the HSA-catalyzed hydrolysis of 4-nitrophenyl acetate [6,11], but also for the cleavage of NphOMy.

Fig. 3 shows the pH dependence of k_{+2}/K_s, k_{+2}, and K_s values for the HSA-catalyzed hydrolysis of NphOMy. Values of kinetic parameters obtained using different buffers at overlapping pH values match very well each other. Values of pK_a modulating the pH dependence of k_{+2}/K_s, k_{+2}, and K_s were determined by data analysis according to Eqs. (6)–(8) [12,13,19]:

$$\text{Log}K_s = -\text{Log}K_s^{lim} + \text{Log}((10^{-pH} + 10^{-pKunl})/(10^{-pH} + 10^{-pKlig})) \quad (6)$$

$$k_{+2} = k_{+2}^{lim}/(1 + (10^{-pH}/10^{-pKlig})) \quad (7)$$

$$k_{+2}/K_s = (k_{+2}/K_s)^{lim}/(1 + (10^{-pH}/10^{-pKunl})) \quad (8)$$

where K_s^{lim}, k_{+2}^{lim}, and $(k_{+2}/K_s)^{lim}$ are the alkaline asymptotes of K_s, k_{+2}, and k_{+2}/K_s, respectively. According to linked functions [12,13,19], the pH dependence of k_{+2}/K_s and k_{+2} reflects the

Table 1
Values of catalytic parameters for the HSA-catalyzed hydrolysis of NphOMy, at 22.0 °C.

pH	[HSA] ⩾ 5 × [NphOMy]			[NphOMy] ⩾ 5 × [HSA]		
	K_s (M)	k_{+2} (s^{-1})	k_{+2}/K_s (M^{-1} s^{-1})	K_s (M)	k_{+2} (s^{-1})	k_{+2}/K_s (M^{-1} s^{-1})
6.9	$(7.2 \pm 0.7) \times 10^{-5}$	$(1.3 \pm 0.1) \times 10^{-4}$	1.8 ± 0.2	$(8.8 \pm 0.8) \times 10^{-5}$	$(1.4 \pm 0.1) \times 10^{-4}$	1.6 ± 0.2
7.5	$(2.6 \pm 0.3) \times 10^{-5}$	$(1.6 \pm 0.2) \times 10^{-4}$	6.2 ± 0.6	$(2.5 \pm 0.3) \times 10^{-5}$	$(1.5 \pm 0.2) \times 10^{-4}$	5.9 ± 0.6
8.1	$(6.3 \pm 0.5) \times 10^{-6}$	$(2.3 \pm 0.2) \times 10^{-4}$	$(3.6 \pm 0.4) \times 10^{1}$	$(6.0 \pm 0.6) \times 10^{-6}$	$(2.1 \pm 0.2) \times 10^{-4}$	$(3.5 \pm 0.4) \times 10^{1}$
8.6	$(3.1 \pm 0.3) \times 10^{-6}$	$(2.2 \pm 0.2) \times 10^{-4}$	$(7.1 \pm 0.7) \times 10^{1}$	$(3.2 \pm 0.3) \times 10^{-6}$	$(2.4 \pm 0.2) \times 10^{-4}$	$(7.4 \pm 0.7) \times 10^{1}$
8.9	$(1.8 \pm 0.2) \times 10^{-6}$	$(2.3 \pm 0.2) \times 10^{-4}$	$(1.3 \pm 0.1) \times 10^{2}$	$(1.6 \pm 0.2) \times 10^{-6}$	$(2.2 \pm 0.2) \times 10^{-4}$	$(1.4 \pm 0.1) \times 10^{2}$
9.5	$(1.6 \pm 0.1) \times 10^{-6}$	$(2.5 \pm 0.3) \times 10^{-4}$	$(1.6 \pm 0.2) \times 10^{2}$	$(1.5 \pm 0.2) \times 10^{-6}$	$(2.6 \pm 0.3) \times 10^{-4}$	$(1.7 \pm 0.2) \times 10^{2}$

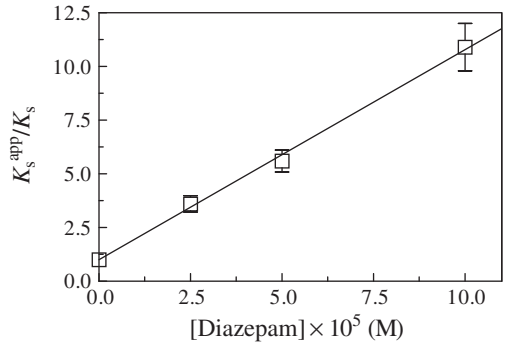

Fig. 2. Competitive inhibitory effect of diazepam on the HSA-catalyzed hydrolysis of NphOMy, at pH 7.5 and 22.0 °C. Data were obtained under conditions where [HSA] ⩾ 5 × [NphOMy]. The continuous line was obtained according to Eq. (5) with $K_i = 1.0 \times 10^{-5}$ M. For details, see text.

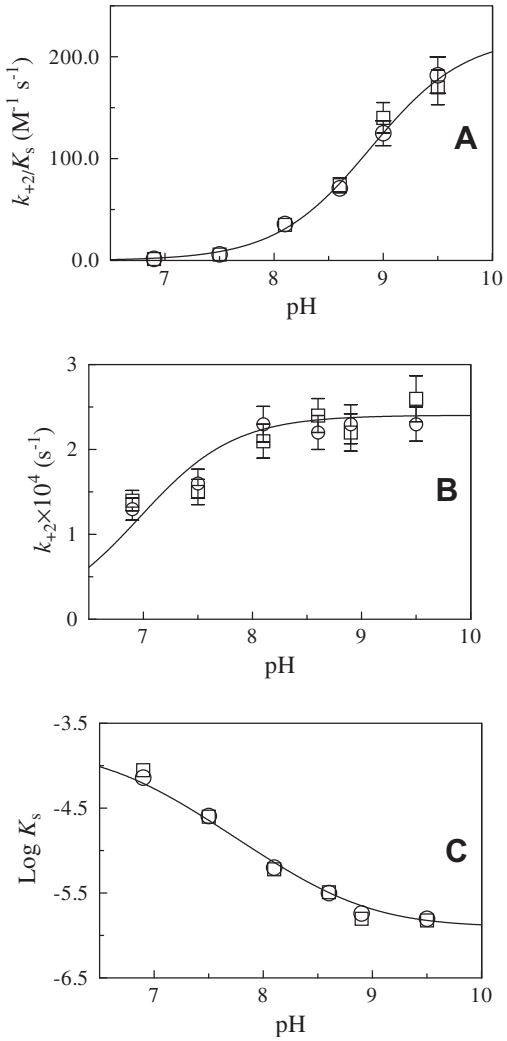

Fig. 3. pH dependence of k_{+2}/K_s (panel A), k_{+2} (panel B), and K_s (panel C) for the HSA-catalyzed hydrolysis of NphOMy, at 22.0 °C. Circles and squares indicate data obtained under conditions where [HSA] ⩾ 5 × [NphOMy] and [NphOMy] ⩾ 5 × [HSA], respectively The continuous lines in panels A, B, and C were obtained from data analysis according to Eqs. (6)–(8) with values of the following parameters: $k_{+2}/K_s - (k_{+2}/K_s)^{lim} = (2.2 \pm 0.2) \times 10^2$ M^{-1} s^{-1} and $pK_{unl} = 8.9 \pm 0.1$; $k_{+2} - k_{+2}^{lim} = (2.3 \pm 0.2) \times 10^{-4}$ s^{-1} and $pK_{lig} = 6.9 \pm 0.2$; and $K_s - K_s^{lim} = (1.4 \pm 0.1) \times 10^{-6}$ M, $pK_{unl} = 8.8 \pm 0.1$, and $pK_{lig} = 6.7 \pm 0.2$. For details, see text.

acid–base equilibrium of a single amino-acid residue in NphOMy-free HSA (*i.e.*, $pK_{unl} = 8.9 \pm 0.1$) and in the HSA:NphOMy complex (*i.e.*, $pK_{lig} = 6.9 \pm 0.2$), respectively. Moreover, the pH dependence of K_s reflects the acidic pK_a-shift of a single amino-acid residue from $pK_{unl} = 8.8 \pm 0.1$ in the NphOMy-free HSA to $pK_{lig} = 6.7 \pm 0.2$ in the HSA:NphOMy complex.

The analysis of the three-dimensional structures of HSA [4,5,15,16,20] and of the chemical modifications by 4-nitrophenyl acetate [5,6,10,11] allows the following considerations. (*i*) The amino acid residue catalyzing the hydrolysis of NphOMy (*i.e.*, undergoing to myristylation) could be Tyr411 located in the FA3-FA4 cleft [16]. In fact, diazepam, inhibiting competitively the HSA-catalyzed hydrolysis of NphOMy (Fig. 2), binds at the center of the FA3-FA4 cleft interacting with the phenoxyl oxygen atom of Tyr411 [16]. It should be noticed that FA3-FA4 is large enough to accommodate two myristate anions, or alternatively larger molecules such as diazepam, ibuprofen or NphOMy (see [5]). (*ii*) Although transient structural changes leading to differences in pK_a values of ionizing group(s) involved in the NphOMy-free HSA and in the HSA catalytic intermediate(s) cannot be directly interpreted on the basis of stereochemical models (see [5]), the acidic pK_a-shift of one apparent ionizing group upon NphOMy binding (Fig. 3) could reflect the interaction between the Tyr411 residue of HSA and NphOMy. Remarkably, the phenoxyl oxygen atom of Tyr411 appears to form a hydrogen bond with the carbonyl oxygen atom of the acylating agent 4-nitrophenyl propionate [11].

As a whole, (ir)reversible chemical modifications affect HSA ligand binding properties (see [5]). Among others, HSA acetylation by aspirin [21] reduces prostaglandin affinity, accelerating the clearance of prostaglandins and serving as an additional mechanism of the aspirin anti-inflammatory effect, increases the affinity of phenylbutazone, and inhibits bilirubin binding [22].

Acknowledgments

This work was partially supported by grants from Ministero dell'Istruzione, dell'Università e della Ricerca of Italy (Università Roma Tre, Roma, Italy; CLAR 2011 to P.A.).

References

[1] T. Peters Jr. (Ed.), All about Albumin: Biochemistry, Genetics and Medical Applications, Academic Press, San Diego and London, 1996.
[2] S. Curry, Beyond expansion: structural studies on the transport roles of human serum albumin, Vox Sang. 83 (Suppl. 1) (2002) 315–319.
[3] M. Fasano, S. Curry, E. Terreno, M. Galliano, G. Fanali, P. Narciso, S. Notari, P. Ascenzi, The extraordinary ligand binding properties of human serum albumin, IUBMB Life 57 (2005) 787–796.
[4] S. Curry, Lessons from the crystallographic analysis of small molecule binding to human serum albumin, Drug. Metab. Pharmacokinet. 24 (2009) 342–357.
[5] G. Fanali, A. di Masi, V. Trezza, M. Marino, M. Fasano, P. Ascenzi, Human serum albumin: from bench to bedside, Mol. Aspects Med. 33 (2012) 209–290.
[6] O. Lockridge, W. Xue, A. Gaydess, H. Grigoryan, S.J. Ding, L.M. Schopfer, S.H. Hinrichs, P. Masson, Pseudo-esterase activity of human albumin: slow turnover on tyrosine 411 and stable acetylation of 82 residues including 59 lysines, J. Biol. Chem. 283 (2008) 22582–22590.
[7] R.F. Chen, Removal of fatty acids from serumalbumin by charcoal treatment, J. Biol. Chem. 242 (1967) 173–181.
[8] M. Sogami, J.F. Foster, Isomerization reactions of charcoal-defatted bovine plasma albumin. The N–F transition and acid expansion, Biochemistry 7 (1968) 2172–2182.
[9] J. Cabrera-Crespo, V.M. Goncalves, E.A. Martins, S. Grellet, A.P. Lopes, I. Raw, Albumin purification from human placenta, Biotechnol. Appl. Biochem 31 (2000) 101–106.
[10] G.E. Means, M.L. Bender, Acetylation of human serum albumin by *p*-nitrophenyl acetate, Biochemistry 14 (1975) 4989–4994.
[11] Y. Sakurai, S.F. Ma, H. Watanabe, N. Yamaotsu, S. Hirono, Y. Kurono, U. Kragh-Hansen, M. Otagiri, Esterase-like activity of serum albumin: characterization of its structural chemistry using *p*-nitrophenyl esters as substrates, Pharmcol. Res. 21 (2004) 285–292.
[12] M.R. Hollaway, E. Antonini, M. Brunori, The pH-dependence of rates of individual steps in ficin catalysis, Eur. J. Biochem. 24 (1971) 332–341.
[13] E. Antonini, P. Ascenzi, The mechanism of trypsin catalysis at low pH proposal for a structural model, J. Biol. Chem. 256 (1981) 12449–12455.

[14] S. Curry, P. Brick, N.P. Franks, Fatty acid binding to human serum albumin: new insights from crystallographic studies, Biochim. Biophys. Acta 1441 (1999) 131–140.
[15] A.A. Bhattacharya, T. Grüne, S. Curry, Crystallographic analysis reveals common modes of binding of medium and long-chain fatty acids to human serum albumin, J. Mol. Biol. 303 (2000) 721–732.
[16] J. Ghuman, P.A. Zunszain, I. Petitpas, A.A. Bhattacharya, M. Otagiri, S. Curry, Structural basis of the drug-binding specificity of human serum albumin, J. Mol. Biol. 353 (2005) 38–52.
[17] P. Ascenzi, M.G. Ascenzi, G. Amiconi, Enzyme competitive inhibition. Graphical determination of *Ki* and presentation of data in comparative studies, 15 (1987) 134–135.
[18] G. Fanali, Y. Cao, P. Ascenzi, V. Trezza, T. Rubino, D. Parolaro, M. Fasano, Binding of δ9-tetrahydrocannabinol and diazepam to human serum albumin, IUBMB Life 63 (2011) 446–451.
[19] L. Peller, R.A. Alberty, Multiple intermediates in steady state enzyme kinetics. I. The mechanism involving a single substrate and product, J. Am. Chem. Soc. 81 (1959) 5907–5914.
[20] S. Sugio, A. Kashima, S. Mochizuki, M. Noda, K. Kobayashi, Crystal structure of human serum albumin at 2.5 Å resolution, Protein Eng. 12 (1999) 439–446.
[21] F. Yang, C. Bian, L. Zhu, G. Zhao, Z. Huang, M. Huang, Effect of human serum albumin on drug metabolism: structural evidence of esterase activity of human serum albumin, J. Struct. Biol. 157 (2007) 348–355.
[22] M.S. Liyasova, L.M. Schopfer, O. Lockridge, Reaction of human albumin with aspirin *in vitro*: mass spectrometric identification of acetylated lysines 199, 402, 519 and 545, Biochem. Pharmacol. 79 (2010) 784–791.